1 Surface-Based Comparisons of Macaque and Human Cortical Organization

David C. Van Essen

In his pioneering architectonic studies of primate cerebral cortex, Brodmann (1909) described a rich mosaic of anatomically distinct cortical areas in both humans and monkeys. He identified 28 neocortical areas in the Old World monkey and 46 in the human, and he used corresponding terminology for most of these areas on the supposition that the similarities in architecture reflected evolutionary homologies. Subsequent studies leave little doubt that the primary sensory and motor areas and their immediate neighbors are indeed homologous in monkeys and humans. On the other hand, the evolutionary relationships are much less clear for most of the remaining expanse of neocortex, mainly because Brodmann's partitioning schemes for both species have been subject to extensive revision over the ensuing century. These revisions are based on many different lines of experimental evidence and are very much a work in progress; consensus has yet to be reached regarding the basic arrangement of cortical areas over most of neocortex in either species. Depending on the criteria used for identifying areas (itself a contentious issue), the total number of cortical areas may approach or exceed 100 areas in the macaque and an even larger number in humans, i.e., double or triple the number enumerated by Brodmann (Van Essen, 2004).

Because human cortex has 10 times the surface area of macaque cortex and plays a key role in many distinctive aspects of human cognition, there presumably are major species differences in cortical functional organization. A priori, these differences might reflect any combination of four basic possibilities:

1. Bigger areas Some areas may have increased in size in humans compared to macaques, thereby providing greater processing power for whatever functions they mediate.
2. Functional divergence Functional specialization of cortical areas may have undergone evolutionary divergence, such that the tasks mediated by homologous cortical areas may be very different in humans compared to macaques.
3. Areas gained or lost Completely new areas may have emerged along the human evolutionary trajectory, analogous to the gene duplication that has often occurred

during evolution of the genome. Alternatively, areas present in a common ancestor may have disappeared in one species but not the other.

4. Rearrangements Topological rearrangement of cortical areas (analogous to "jumping genes" in chromosomal DNA) may have occurred along one evolutionary trajectory but not the other.

To distinguish among these possibilities requires accurate maps of cortical organization in each species plus objective methods for making comparisons between maps. A fundamental challenge in mapping the cortex arises from cortical convolutions—both their existence and the dramatic species differences in the pattern of convolutions. Despite its convolutions, the cortex is a continuous sheet of tissue, topologically equivalent to a disc, and it can be represented by explicit surface reconstructions that capture the intricacies of cortical shape. Surface reconstructions facilitate visualization of many aspects of cortical organization that are difficult to decipher when viewing a series of slices through the brain. Moreover, the differences in cortical shape can be eliminated by mapping each cortical surface to a standard configuration, such as a sphere. One sphere can then be registered to another, constrained by landmarks that reflect known or suspected homologies. Consequently, surface-based registration provides a general and powerful strategy for analyzing species differences in cortical organization.

This chapter illustrates how surface-based visualization and interspecies registration can help clarify a number of specific issues and controversies regarding the functional organization of human and macaque cerebral cortex. The analysis is focused on two sets of areas situated at opposite ends of the hemisphere: orbital and medial prefrontal cortex (OMPFC) and visuotopically organized portions of occipital visual cortex. These choices are based on the availability of detailed maps of cortical organization in both regions for both species obtained using modern experimental approaches.

To set the stage for this analysis, figure 1.1 shows surface reconstructions of macaque and human right cerebral hemispheres, generated from high-resolution structural MRI data using the SureFit segmentation method and visualized using Caret software (Van Essen et al., 2001, 2004). The surfaces are displayed in five standard configurations; the shading on each map represents cortical depth (deeper is darker), which provides a convenient measure of the original cortical shape. The fiducial surfaces (panels A, F) represent the shape of the cortex, including all of the convolutions. The inflated maps (panels B, G) retain the approximate shape of the brain but smooths out all but the deepest folds. The spherical maps (panels C, H) provide a geometrically precise representation that is the substrate for registration between species. It also provides the basis for surface-based coordinates that concisely and objectively specify locations on the cortical surface, as indicated by the latitude (black) and longitude (gray)

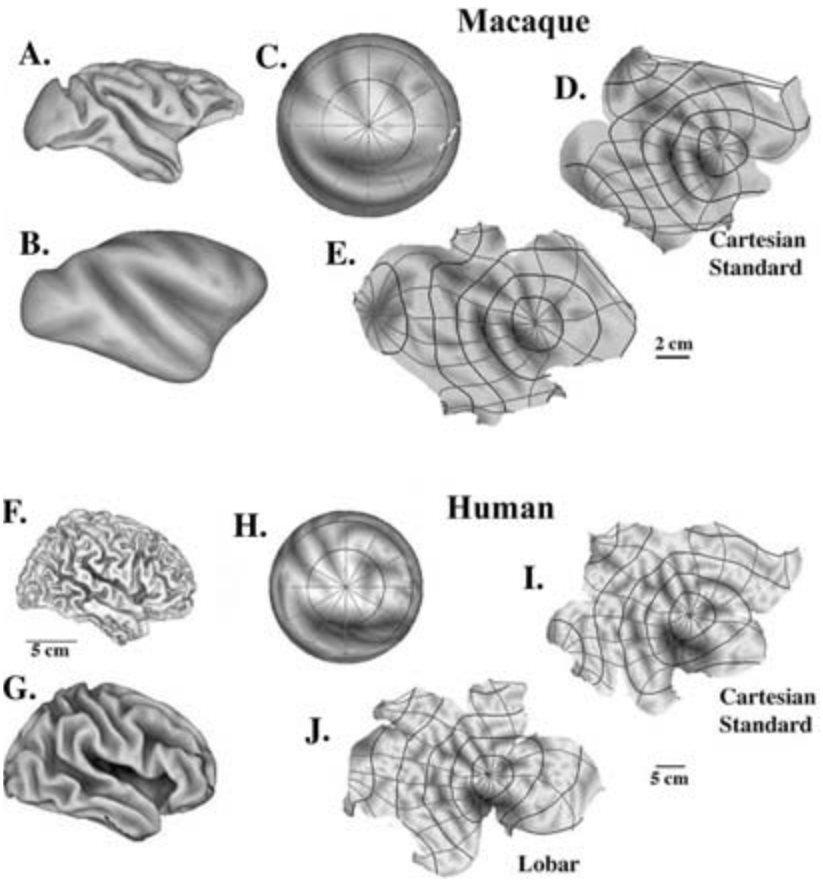

Figure 1.1

Surface-based atlases of human and macaque cortex. (*A–E*) Right cerebral hemisphere of the macaque F99UA1 atlas (Van Essen et al., 2004). (*F–J*) Right cerebral hemisphere of the human Colin atlas (Van Essen, 2002). Both atlas surfaces are shown in five configurations: fiducial, inflated, spherical, Cartesian standard flat, and lobar flat. The spherical and flat maps include latitude and longitude isocontours used for defining spherical coordinates.

isocontours on each spherical map in figure 1.1. The flat maps allow the entire cortical sheet to be seen in a single view without severe distortions (akin to flat maps of the earth's surface). Panels D and I show the commonly used Cartesian standard configuration; panels E and J show the "lobar" configuration that is better suited for the data analyzed here because it avoids cuts in occipital and frontal lobes. Each of the flat maps contains a different pattern of areal distortions relative to the fiducial surface. Various differences that are discussed below regarding the relative sizes of particular regions and areas are based on surface area measurements of the fiducial surface, not on the sometimes deceptive surface areas on the flat maps.

The macaque atlas map in figure 1.2A–D (see also plate 1) shows visuotopically organized areas in occipital cortex and posterior temporal parietal cortex, as identified in the Felleman and Van Essen (1991) partitioning scheme. The human atlas map (figure 1.2F–I) includes visuotopic areas from fMRI mapping studies (Hadjikhani et al., 1998; see Van Essen, 2004). In addition, panels E and J show alternate schemes for ventral occipitotemporal cortex in macaque and human. Both atlases include maps of architectonic areas in orbital and medial prefrontal cortex (OMPFC), identified using a combination of cytoarchitecture, myeloarchitecture, and immunocytochemistry (Carmichael & price, 1994; Ferry, Öngür, An, & Price, 2000; Öngür and Price, 2000; Öngür, Ferry, & Price, 2003). The atlas configurations include lateral and medial views of the fiducial surface (figure 1.2, A, B, F, G), inflated maps viewed from an anteroventral perspective (figure 1.2 C, H), and flat maps in the lobar configuration to avoid cuts where the areas have been mapped (figure 1.2 D, I).

All of the labeled regions shown in figure 1.2 differ from one another in significant respects, but not all of them are generally accepted as genuine cortical areas. In the terminology used here (see also Lewis and Van Essen, 2000), a cortical area refers to a well-defined region identifiable by one or more attributes that both unify the region and distinguish it from surrounding regions. A zone signifies a region in which one or more consistent regional differences have been reported, but may not warrant consideration as separate areas. A subdivision is a more neutral term, signifying a noncommittal label as to whether the region is an area or a zone.

The cortical areas shown in figure 1.2A–I were initially charted on individual hemispheres that had been analyzed using anatomical or functional methods. They were registered to the atlas maps using surface-based registration (Van Essen et al., 2001; Van Essen, Harwell, Hanlon, & Dickson, 2004), with geographic landmarks as constraints for the registration. Owing to the well-known individual variability in the location of areal boundaries relative to nearby geographic landmarks, there is inherently some uncertainty associated with the location of all areas on the atlas maps.

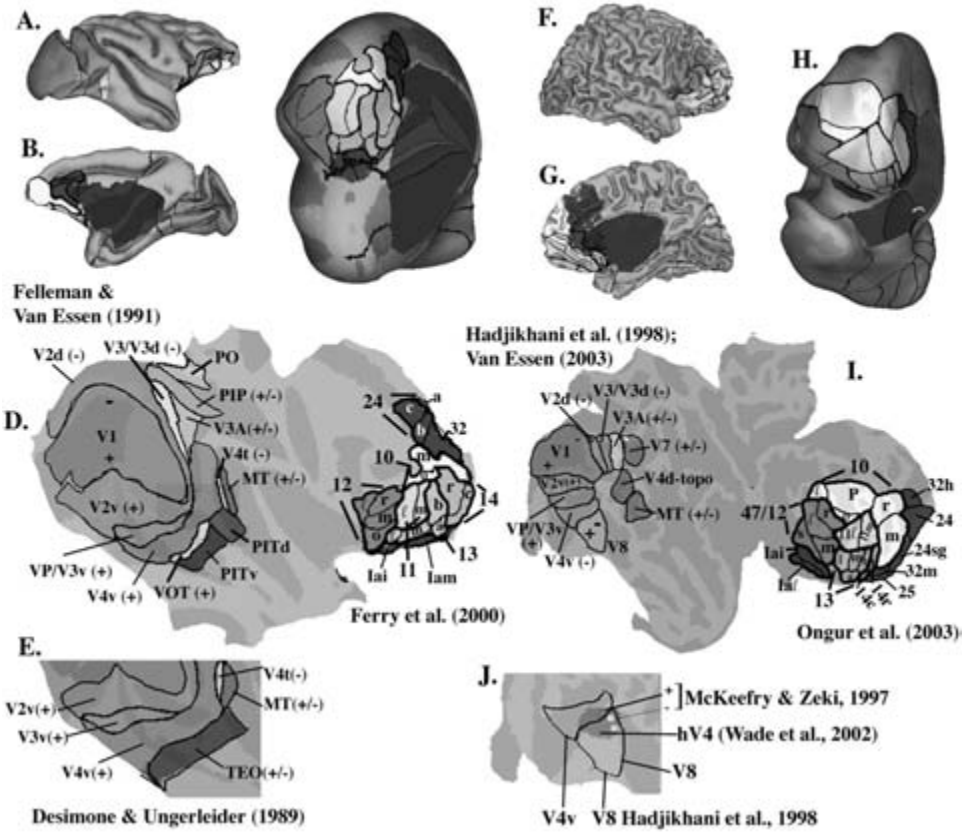

Figure 1.2

Visuotopic and orbitomedial prefrontal cortex (OMPFC) subdivisions of macaque and human cortex. (*A–D*) Fiducial (lateral and medial), inflated, and lobar flat map views of the macaque atlas with visuotopic areas (Felleman & Van Essen, 1991) and OMPFC areas (Ferry et al., 2000, case om 43). (*E*) Visual areas from Desimone and Ungerleider (1989) on a flat map of just ventral occipitotemporal cortex. (*F–I*) Fiducial, inflated, and lobar fat map views of the human atlas with visuotopic areas (Hadjikhani et al., 1998; see Van Essen, 2004) and OMPFC areas (Öngür et al., 2003; composite map generated as an average of three individual right hemispheres). (*J*) Human V4 as delineated by Wade et al. (2002, their figure 9b, case, A.W. right hemisphere) and by McKeefry and Zeki (1997; red, center of upper-field activation; green, center of lower-field activation). The visuotopic maps were registered using a 2-D registration algorithm applied to published images of flat maps. The OMPFC maps were registered by mapping the prefrontal surface reconstructions to a partial sphere, then registering this to the atlas sphere. In all cases, geographic (sulcal) landmarks were used to constrain the registration. Data sets used in generating this figure and figures 1.1–1.4 can be accessed via http://brainmap.wustl.edu:8081/sums/archivelist.do?archive_id=636599. See plate 1 for color version.

OMPFC Areas

In the macaque, Ferry et al. (2000) charted 20 orbitofrontal areas, as shown in figure 1.2A–D for one individual case mapped to the atlas map (see figure legend for details). As indicated by the coloring scheme and by the thicker borders around each area complex, most of these involve finer-grained subdivisions of Brodmann's numbering scheme, as modified by Walker (1940) and Petrides and Pandya (2002). In human cortex, Öngür et al. (2003) charted 24 orbitofrontal subdivisions, shown in figure 1.2B after mapping to the atlas. In general, there are many similarities in the layout of areas in the two species, but some major differences as well. The most lateral cluster (left on the flat maps), includes four subdivisions of macaque area 12 and of human area 47/12, with both sets colored red to reflect the presumed homologies. More medial and ventral are clusters that include two subdivisions of area 11 (green), four of area 13 (light blue), and two of area 14 (orange). These differ in relative size (e.g., 14r and 14c are much smaller on the human map). Anterior and more dorsal area is the area 10 complex (yellow), whose five subdivisions in humans (10p, 10o, 10r, 10m, and 10l) occupy 4.5 percent of neocortical surface areqa, which is three-fold greater than the 1.4 percent occupied by the two subdivisions (10m, 10o) in the macaque. Medially is a complex of areas that includes subdivisions of areas 24, 25, and 32. The topological (neighborhood) relationships between different areas are generally similar in macaque and human. There are a few minor differences, comparable to the differences in individual hemispheres mapped within the same species (Ferry et al., 2000); it remains to be determined whether this reflects genuine variability in map topology versus experimental uncertainties in charting areal boundaries.

Visuotopic Subdivisions

In the macaque, cortex that is predominantly or exclusively visual in function occupies more than half of the total cortical surface area. There is evidence for up to 40 visual subdivisions (areas plus zones; Lewis and Van Essen, 2000) but considerably fewer in various other partitioning schemes (see Van Essen, 2004). Orderly visuotopic maps occur in many visual areas, particularly in occipital cortex. Figure 1.2 shows 16 visuotopic subdivisions of the Felleman and Van Essen (1991) scheme, in which the visuotopic maps progress from extremely precise and fine-grained in area V1 to very coarse in the posterior inferotemporal complex (PITd and PITv). Area V1 contains a complete map of the contralateral visual hemifield and is bounded by a representation of the vertical meridian. Area V2 shares the vertical meridian representation with V1 and includes a split representation of the horizontal meridian along the anterior boundaries of its upper field (+) and lower field (–) representations. Of the remaining visuotopic subdivisions, some have complete representations (indicated by +/– on the

flat map) but other representations are incomplete (+ or – on the map). Whether the partial-field representations constitute distinct visual areas is controversial (see below). The human map includes 11 visuotopically organized subdivisions, including several partial-field representations. The coloring scheme indicates potential correspondences between macaque and human, but not all of these necessarily represent genuine homologies.

The three clearest homologies are for areas V1, V2, and MT. In both species, V1 is the largest single area, but as a fraction of total cortex it is several times larger in the macaque than human cortex (10 percent vs. 3 percent). V2 is the second-largest area in both species. MT (also known as V5) is a much smaller area, distinguished by a high incidence of direction selectivity in the macaque (Van Essen et al., 1981) and by motion-selective PET and fMRI activations in humans (Watson et al., 1993; Hadjikhani et al., 1998). The map of the human motion-specific focus is identified as MT+ because it likely includes some of the adjoining motion-responsive MST complex. In both species MT has a similar visuotopic organization (Van Essen, Maunsell & Bixby, 1981; Huk, Dougherty, & Heeger, 2002).

In both the human and the macaque, V2 is adjoined dorsally by a lower-field representation and ventrally by an upper-field representation, referred to here as V3d and V3v respectively, rather than the alternate nomenclature of V3 and VP. In the macaque, V3d and V3v are reported to differ in some aspects of architecture, function, and connectivity (Van Essen, Newsome, Maunsell, & Bixby, 1986), though the magnitude of these dorsoventral asymmetries is controversial (Lyon & Kaas, 2002). Recent fMRI studies support the hypothesis of functional asymmetries between V3d and V3v (Tsao et al., 2003; Denys et al., 2003), but more detailed analyses are needed to assess the magnitude, nature, and significance of such asymmetries. The issue of whether V3d and V3v are separate areas or subdivisions of a unified V3 is to a large extent semantic, and the debate could be regarded as a tempest in a teapot if it applied only to V3d and V3v. However, analogous issues arise in the analysis of V4 and adjoining regions (see below), making the conceptual distinction of greater import.

In the macaque, both V3d and V3v are generally narrower than V2 when charted anatomically and neurophysiologically, consistent with their coarser visuotopic organization and larger receptive field sizes (Van Essen et al., 1986; Gattass, Sousa, & Gross, 1988). In contrast, fMRI-based estimate suggest that V3d and V3v are comparable in width to V2, both in the macaque (Brewer, Press, Logothetis, & Wandell, 2002; Fize et al., 2003) and in humans (figure 1.2B; Hadjikhani, Liu, Dale, Cavanagh, & Tootell, 1998; Wade, Brewer, Rieger, & Wandell, 2002; Dougherty et al., 2003). However, the fMRI-based estimates of areal boundaries in both species may be significantly biased as a consequence of the limited spatial resolution of fMRI with current methodology, and such biases could have a significant impact on estimated areal dimensions and surface areas.

V3A in both macaque and human involves a complete upper and lower field representation, albeit coarser and irregular. In the macaque V3A is adjoined medially by areas PIP and PO (Colby, Gattass, Olson, & Gross, 1988). In humans V3A is adjoined dorso-anteriorly by area V7 (Press et al., 2001).

In the macaque, area V4 includes a dorsal lower-field representation and a ventral upper-field representation that have been mapped physiologically (Gattass et al., 1988; Boussaud et al., 1991) and by fMRI (Brewer et al., 2002; Fize et al., 2003). Fize et al. (2003) describes a visuotopic asymmetry, in which the horizontal meridian representation forms the anterior boundary of V4 ventrally but not dorsally. V4t is a narrow strip lying between dorsal V4 and MT (Gattass et al., 1988) that represents lower fields, but it has not been resolved using fMRI. VOT is a narrow upper-field representation that has been mapped neurophysiologically (Van Essen et al., 1990; see also Boussaud et al., 1991) and by callosal connectivity (Van Essen et al., 1982) and fMRI mapping (Brewer et al., 2002, their figure 14). It lies anterior to V4v and posterior to the posterior inferotemporal complex, which includes two subdivisions (PITd and PITv) that each have a crude representation of upper and lower fields (Van Essen et al., 1990). In contrast, Boussaud et al. (1991) described TEO as a subdivision that subsumes VOT plus part of the adjoining PIT complex (figure 1.2E).

The location and nature of human area V4 remains controversial, with conflicting and at times confusing views regarding facts, terminology, and interpretation. Several studies have mapped an upper-field representation and identified it as human V4v because it lies in a corresponding location just anterior to V3v (i.e., a "topolog" of macaque V4v) and has a similar visuotopic organization (Sereno et al., 1995; DeYoe et al., 1996: Hadjikhani et al., 1998). These studies did not find a corresponding map of lower fields that would qualify as V4d. Hadjikhani et al. (1998) charted a separate representation of upper and lower fields that they identified as V8, lying antero-lateral to V4v (centered on [–38°, –122°] latitude and longitude on the atlas map). The foveal representation of V8 was clearly separate from that for V4v in one case, but the eccentricity mapping was ambiguous in other cases. The general region dorsolateral to V4v and posterior to MT has been variously identified as KO, LO, V3B LOC/LOP, or V4d-topo (Van Oostende et al., 1997; Smith et al., 1998; Tootell and Hadjikhani, 2001; Tsao et al., 2003). The V4d topolog (V4d-topo) name reflects its location relative to V2, V3A, V4v and MT, but its visuotopic organization is crude and does not match that of macaque V4d, nor is it mirror-symmetric to human V4v (Tootell and Hadjikhani, 2001). Thus, for both species it is an open question whether V4v and V4d/V4d-topo should be regarded as distinct areas or asymmetric components of a single area.

An alternative scheme (figure 1.2J) posits that human area V4 is a color-specific area restricted to ventral occipito-temporal cortex (Lueck et al., 1989; McKeefry & Zeki, 1997). Based on the Talairach stereotaxic coordinates of PET activation centers, its

upper-field representation maps to [–40°, –135°] on the atlas map (red in figure 1.2J) and its lower-field representation maps to [–34°, –135°] (green in figure 1.2J) with both foci close to the boundary of V8/V4v of Hadjikhani et al. (1998). However, in contrast to the situation with MT, evidence for a human color-specific activation provides only weak support for a homology with macaque V4 because macaque V4 is not specialized for color processing in the same way that MT is specialized for motion processing (Girard, Lomber, & Bullier, 2002; Cowey et al., 2001; see Felleman and Van Essen, 1991). Wade et al. (2002) mapped a representation of upper and lower fields in the same general region (blue in figure 1.2J for one of their individual cases mapped to the atlas). They consider the lower-field representation to be part of a single area, hV4, whose upper field includes V4v but not the upper-field component of V8 in the Hadjikhani et al. (1998) scheme. This interpretation is in accord with the McKeefry and Zeki (1997) scheme, but the data appear to be consistent also with the Hadjikhani et al. (1998) scheme for V8, given the noisiness and mapping uncertainties in the published data. Altogether, there is a pressing need for accurate, higher-resolution visuotopic maps in order to address the ambiguities and apparent discrepancies across studies. In the meantime, though, valuable additional insights can be obtained by comparing the published maps more closely using surface-based registration.

Surface-Based Registration

A key to interspecies registration is to identify a set of landmarks that can be reliably identified in both atlas maps and are highly likely to reflect genuine evolutionary homologies. The landmarks indicated in figure 1.3A and B (see plate 2) include early visual areas (V1, V2, and MT), other primary sensory areas (A1, olfactory, and gustatory cortex and the border between areas 3 and 4), the hippocampus, the olfactory sulcus, and additional landmarks along the natural boundary of cortex on the medial wall of the hemisphere. The relative positions of these landmarks (figure 1.3A–B) imply that highly nonuniform scaling must occur in several regions in order to achieve registration between the two maps. For example, V1 and V2 are a much smaller fraction of human compared to macaque cortex; the gap between MT and A1 is much larger on the human than the macaque map, and the gap between the frontal eye fields (FEF) and the boundary between somatosensory and motor cortex (areas 3 and 4) is much smaller on the human than the macaque map. These interspecies differences in relative location of functionally based landmarks greatly exceed the spatial uncertainties associated with each of the landmarks on the atlas maps, even for landmarks such as the FEF that are difficult to delineate with great accuracy in humans.

The landmark borders in figure 1.3 were drawn on flat maps and projected to the spherical maps. Registration was then carried out using an algorithm that deforms one spherical map to another, bringing the macaque landmarks into register with the

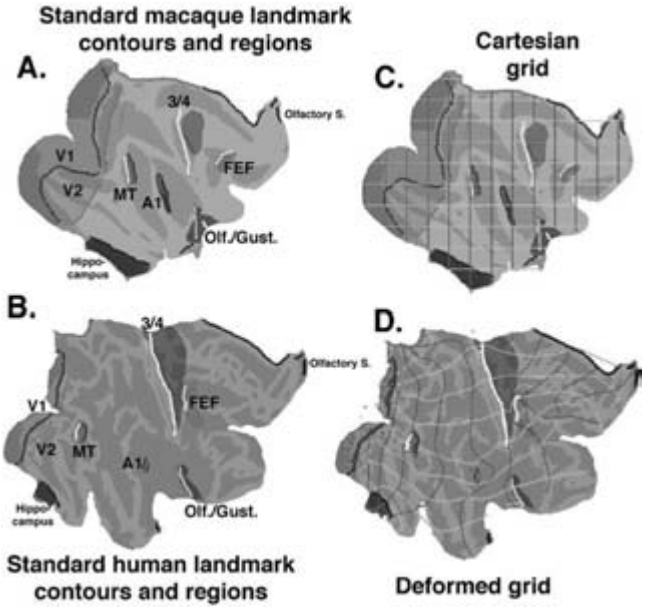

Figure 1.3
Landmarks used for registration between macaque and human right hemispheres. (*A*) Landmark areas and boundaries on the macaque atlas flat map (Cartesian standard). (*B*) Corresponding areas and boundaries on the human atlas flat map. (*C*) Cartesian grid on the macaque flat map. (*D*) Deformed macaque grid lines on the human map. (Reproduced with permission from Van Essen et al., 2004.) See plate 2 for color version.

human landmarks while minimizing shear and areal distortion in the intervening regions (Van Essen et al., 2004). A Cartesian grid on the macaque flat map (figure 1.3C) was projected to the macaque sphere, passively deformed to the human sphere, and projected to the human flat map (figure 1.3D). As expected from the relative locations of landmarks, the deformed grid is relatively compressed in occipital cortex and in posterior frontal cortex, whereas it is greatly expanded over much of parietal, temporal, and frontal cortex. For any given pair or triplet of landmarks, the registration algorithm results in relatively uniform expansion in the intervening region. If this results in good alignment between monkey and human areas that are known or suspected to be homologous in these intervening regions, then there is no need to invoke additional landmarks. If, on the other hand, the correspondence is poor, then additional or alternate landmarks can be explored.

Figure 1.4 (plate 3) shows the deformed macaque visuotopic and orbitofrontal areas, with the boundaries of the human areas overlaid. These are displayed on ventral, lateral, and medial views of the inflated surfaces (figure 1.4A–C), on a Cartesian stan-

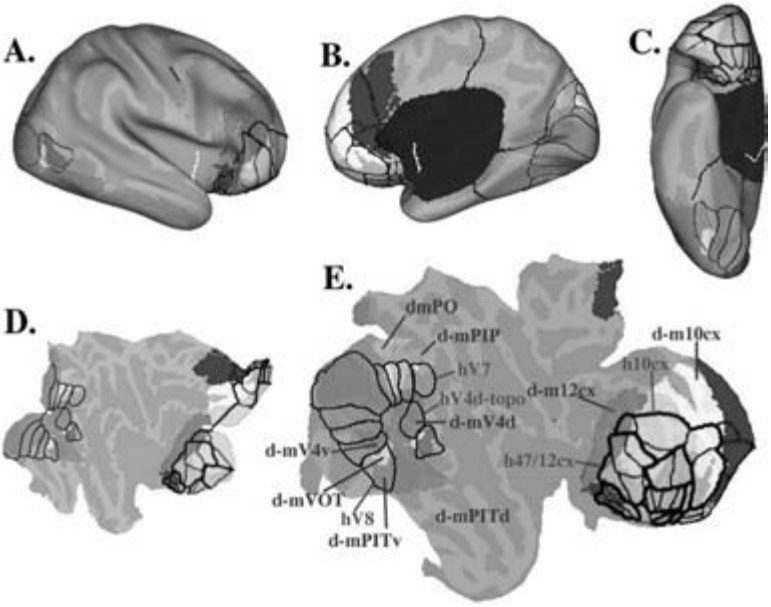

Figure 1.4
Deformed macaque areas (painted on surface) plus human areal boundaries (black contours) on the human atlas surface. (*A–C*) Ventral, lateral, and medial views of inflated configuration. (*D*, *E*) Cartesian standard and lobar flat map views. The prefix "d-m" signifies deformed macaque and is indicated by green labels for selected visual subdivisions (d-mVOT, etc.) and for OMPFC area complexes (d-m12cx, etc.). Selected human areas are identified by red labels and an "h" prefix (hV8, etc.). See plate 3 for color version.

dard flat map (figure 1.4D), and on a lobar cut flat map (figure 1.4E). In general, the deformed macaque OMPFC area complexes (d-m12cx, d-m10cx, etc.) occupy a substantially larger expanse on the human map (18 percent of total fiducial surface area) than do the corresponding human areas (about 11 percent of total surface area). Their expanded position occupies a broad swath of posterior and dorsal prefrontal cortex that includes portions of human areas 9, 45, 46, and 47. This mismatch between human and deformed macaque OMPFC areas strongly suggests a nonuniform expansion of prefrontal cortex in humans compared to macaques, in which dorsolateral and dorsomedial PFC expanded more than the OMPFC areas. This hypothesis can be made explicit by incorporating additional constraints, based on the boundaries of the OMPFC areas themselves. More generally, landmarks for homologies can be incorporated wherever a differential expansion of cortical regions is known or suspected. Of course, another option is to hypothesize that some of the proposed OMPFC areal homologies between human and macaque are not valid and to explore alternative candidate homologues suggested by other studies.

In visual cortex, deformed macaque V1, V2, and MT align well with their respective human counterparts, as, expected because these areas were used as landmarks. Deformed macaque V3d and V3v are narrower than their human counterparts, which may in part reflect an artifactual overestimate of the width of human V3d/v (see above). Deformed macaque V3A overlaps significantly with human V3A, consistent with their presumed homology. In contrast, human V7 does not overlap with deformed macaque PIP or PO, suggesting that human V7 lacks a known visuotopically organized homolog in the macaque and that macaque PIP and PO lack known visuotopically organized homologues in humans.

In ventral and lateral occipital cortex, deformed macaque V4v and V4d overlap extensively with human V4v and V4d-topo respectively, consistent with the homologies proposed by Tootell and Hadjikhani (2001). Deformed macaque VOT and PITv (but not PITd) lie mainly within human V8. In contrast, deformed macaque V4d (centered at [–24°, –134°]) longitude and latitude is very distant from human V8 and from the lower-field representation of human V4 (centered at [–33°, –134°]) proposed by McKeefry and Zeki (1997) and Wade et al. (2002). Hence, in order for this proposed homology to be valid, it would be necessary to invoke either (1) the emergence of a large cortical domain in human occipital cortex (lying between V2d, V3d, V3A, MT, and V4v) that has no homolog in the macaque, or (2) a major rearrangement in the topological relationships of homologous areas in the two species. While not impossible, neither of these possibilities is as plausible as the proposed homology between human V4d-topo and macaque V4d.

Comparing Macaque and Human Cerebellum

The cerebellum provides an interesting substrate for demonstrating the generality of surface-based interspecies comparisons, because cerebellar cortex is another sheetlike structure whose morphology and functional organization differs in many ways from cerebral cortex. Although cerebellar cortex is thinner and even more convoluted than cerebral cortex, it has recently been possible to generate accurate surface reconstructions of the full set of cerebellar lobules and lamellae and many of its fine-grained folia in both the human and macaque atlases (Van Essen, 2002). Figure 1.5 shows these cerebellar surface reconstructions in fiducial, spherical, and flat map configurations for macaque (figure 1.5A) and human (figure 1.5C). The cerebellar lobules are indicated by roman numerals alongside each flat map. As in figure 1.1, the shading on each map represents depth below the external hull. The elongation of the flat maps (particularly in the macaque) reflects the parallel folds along the cerebellar midline (center strip) and of the cerebellar hemispheres.

Figure 1.5B shows the results of deforming from macaque to human cerebellum using lobular boundaries as landmarks and spherical registration to constrain the

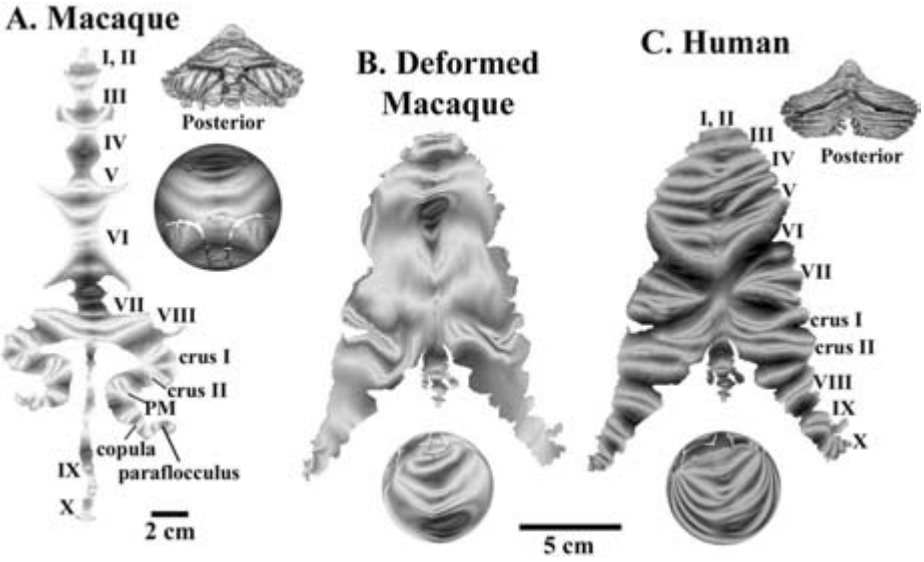

Figure 1.5
Macaque and human cerebellar maps. (*A*) Fiducial, spherical, and flat maps of macaque cerebellar cortex, with shading representing depth below the external hull of the cerebellum (lobules I–X and other geographic landmarks are shown on right). (*B*) Deformed macaque depth map after registration to the human spherical map (below) and flat map (above) using lobule boundaries to constrain the registration. (*C*) Fiducial, spherical, and flat maps of human cerebellar cortex. Data sets are accessible via http://brainmap.wustl.edu:8081/sums//archivelist.do?archive_id=632425.

deformation. Using these anatomical landmarks results in a pattern of differential expansion that is considerably greater than for cerebral cortex. Although the amount of experimental data on the cerebellar atlases is currently far less than for cerebral cortex, this approach will facilitate a wide variety of comparisons. For example, connectivity data obtained in the macaque (e.g., Kelly & Strick, 2003) can be mapped to the atlas, deformed to the human map and compared to fMRI data that have been mapped to the human cerebellar atlas. This should reveal whether functionally based subdivisions map to corresponding lobules in the macaque and human cerebellum.

Extending the Comparisons

The analyses and interspecies comparisons presented in this chapter can be extended in an open-ended way to all regions of cerebral and cerebellar cortex. They can be used to evaluated candidate homologies involving a wide variety of partitioning

schemes and many types of neuroimaging and other experimental data. Recent advances in brain-mapping software and databases allow this to be done in a flexible and efficient way. The current macaque and human surface-based atlases contain extensive data besides that illustrated in this chapter, including multiple partitioning schemes (14 for the macaque, 3 for human), connectivity and neurophysiology data in the macaque, and fMRI data (especially for human). The atlas data sets are accessible via the SumsDB database (http://brainmap.wustl.edu:8081/sums). Caret surface visualization software is freely available (http://brainmap.wustl.edu/caret) and runs on standard PC and Mac workstation platforms. This software also provides tools for mapping additional data to the atlas and entering data into the database. The specific data illustrated in this chapter can be downloaded from SumsDB (see URLs in figure 1.2 and figure 1.5 legends) and viewed in Caret.

In short, the stage is set for a fresh approach to studying human and macaque cortical organization that can capitalize on the explosion of experimental data being generated for both species. This provides an exciting opportunity to elucidate major commonalities and the nature of species differences that make us uniquely human.

Acknowledgments

Supported by a Human Brain Project/Neuroinformatics research grant funded jointly by the National Institute of Mental Health, National Science Foundation, National Cancer Institute, National Library of Medicine and the National Aeronautics and Space Administration (R01 MH60976-06), and The National Partnership for Advanced Computational Infrastructure (NPACI). I thank Dr. J. Price for comments on the manuscript, Susan Danker for assistance with manuscript preparation, and John Harwell, Donna Hanlon, James Dickson, and Heather Drury for development of Caret, SureFit, and SumsDB software.

References

Boussaud, D., Desimone, R., & Ungerleider, L. G. (1991). Visual topography of area TEO in the macaque. *Journal of Comparative Neurology*, *306*, 554–575.

Brewer, A. A., Press, W. A., Logothetis, N. K., & Wandell, B. A. (2002). Visual areas in macaque cortex measured using functional magnetic resonance imaging. *Journal of Neuroscience*, *22*, 10416–10426.

Brodmann, K. (1909). *Vergleichende Lokalisationslehre der Grosshirnrinde in ihren Prinzipien dargestellt auf Grund des Zellenbaues*. Leipzig: J. A. Barth.

Carmichael, S. T., & Price, J. L. (1994). Architectonic subdivision of the orbital and medial prefrontal cortex in the macaque monkey. *Journal of Comparative Neurology*, *346*, 366–402.

Colby, C. L., Gattass, R., Olson, C. R., & Gross, C. G. (1988). Topographic organization of cortical afferents to extrastriate visual area PO in the macaque: a dual tracer study. *Journal of Comparative Neurology*, *269*, 392–413.

Cowey, A., Heywood, C. A., & Irving-Bell, L. (2001). The regional cortical basis of achromatopsia: a study on an achromatopsic patient. *European Journal of Neuroscience*, *14*, 1555–1566.

Denys, K., Vanduffel, W., Fize, D., Nelisen, K., Peuskens, H., Van Essen, D., & Orban, G. A. (2003). The processing of visual shape in the cerebral cortex of human and non-human primates: An fMRI study. In preparation.

Desimone, R., & Ungerleider, L. (1989). Neural mechanisms of visual processing in monkeys. In F. Boller & J. Graman (Eds.), *Handbook of Neuropsychology* (pp. 267–299). Amsterdam: Elsevier.

DeYoe, E. A., Carman, G., Bandetinni, P., Glickman, S., Wieser, J., Cox, R., Miller, D., & Neitz, J. (1996). Mapping striate and extrastriate visual areas in human cerebral cortex. *Proceedings of the National Academy of Sciences*, *93*, 2382–2386.

Dougherty, R. F., Koch, V. M., Brewer, A., Fischer, B., Modersitzki, J., & Wandell, B. (2003). Visual field representations and locations of visual areas V1/2/3 in human visual cortex. *Journal of Vision*, *3*, 1–3.

Felleman, D. J., & Van Essen, D. C. (1991). Distributed hierarchical processing in primate cerebral cortex. *Cerebral Cortex*, *1*, 1–47.

Ferry, A. T., Öngür, D., An, X., & Price, J. L. (2000). Prefrontal cortical projections to the striatum in macaque monkeys: evidence for an organization related to prefrontal networks. *Journal of Comparative Neurology*, *425*, 447–470.

Fize, D., Vanduffel, W., Nelissen, K., Denys, K., Chef d'Hotel, C., Faugeras, O., & Orban, G. A. (2003). The retinotopic organization of primate dorsal V4 and surrounding areas: A functional magnetic resonance imaging study in awake monkeys. *Journal of Neuroscience*, *23*, 7395–7406.

Gattass, R., Sousa, A. P. B., & Gross, C. G. (1988). Visuotopic organization and extent of V3 and V4 of the macaque. *Journal of Neuroscience*, *8*, 1831–1845.

Girard, P., Lomber, S. G., & Bullier, J. (2002). Shape discrimination deficits during reversible deactivation of area V4 in the macaque monkey. *Cerebral Cortex*, *12*, 1146–1157.

Hadjikhani, N., Liu, A. K., Dale, A. M., Cavanagh, P., & Tootell, R. B. H. (1998). Retinotopy and color sensitivity in human visual cortical area V8. *Nature Neuroscience*, *1*, 235–241.

Huk, A. C., Dougherty, R. F., & Heeger, D. J. (2002). Retinotopy and functional subdivision of human areas MT and MST. *Journal of Neuroscience*, *22*, 7195–7205.

Kelly, R. M., & Strick, P. L. (2003). Cerebellar loops with motor cortex and prefrontal cortex of a non-human primate. *Journal of Neuroscience*, *23*, 8432–8444.

Lewis, J. W., & Van Essen, D. C. (2000). Architectonic parcellation of parieto-occipital cortex and interconnected cortical regions in the Macaque monkey. *Journal of Comparative Neurology*, *428*, 79–111.

Lueck, C. J., Zeki, S., Friston, K. J., Deiber, M. P., Cope, P., Cunningham, V. J., Lammertsma, A. A., Kennard, C., & Frackowiak, R. S. J. (1989). The colour centre in the cerebral cortex of man. *Nature*, *340*, 386–389.

Lyon, D. C., & Kaas, J. H. (2002). Evidence for a modified v3 with dorsal and ventral halves in macaque monkeys. *Neuron*, *33*, 453–461.

McKeefry, D. J., & Zeki, S. (1997). The position and topography of the human colour centre as revealed by functional magnetic resonance imaging. *Brain*, *120*, 2229–2242.

Öngür, D., Ferry, A. T., & Price, J. L. (2003). Architectonic subdivision of the human orbital and medial prefrontal cortex. *Journal of Comparative Neurology*, *460*, 425–449.

Öngür, D., & Price, J. L. (2000). The organization of networks within the orbital and medial prefrontal cortex of rats, monkeys and humans. *Cerebral Cortex*, *10*, 206–219.

Petrides, M., & Pandya, D. N. (2002). Comparative cytoarchitectonic analysis of the human and the macaque ventrolateral prefrontal cortex and corticocortical connection patterns in the monkey. *European Journal of Neuroscience*, *16*, 291–310.

Press, W. A., Brewer, A. A., Dougherty, R. F., Wade A. R., & Wandell, B. A. (2001). Visual areas and spatial summation in human visual cortex. *Vision Research*, *41*, 1321–1332.

Sereno, M. I., Dale, A. M., Reppas, J. B., Kwong, K. K., Belliveau, J. W., Brady, T. J., et al. (1995). Borders of multiple visual areas in humans revealed by functional magnetic resonance imaging. *Science*, *268*, 889–893.

Smith, A. T., Greenlee, M. W., Singh, K. D., Kraemer, F. M., & Hennig, J. (1998). The processing of first- and second-order motion in human visual cortex assessed by functional magentic resonance imaging (fMRI). *Journal of Neuroscience*, *18*, 3816–3830.

Tootell, R. B. H., & Hadjikhani, N. (2001). Where is "dorsal V4" in human visual cortex? Retinotopic, topographic and functional evidence. *Cerebral Cortex*, *11*, 298–311.

Tsao, D. Y., Vanduffel, W., Sasaki, Y., Fize, D., Knutsen, T. A., Mandeville, J. B., et al. (2003). Stereopsis activates V3A and caudal intraparietal areas in macaques and humans. *Neuron*, *39*, 555–568.

Van Essen, D. C. (2002). Surfacebased atlases of cerebellar cortex in human, macaque, and mouse. *Annals of the New York Academy of Sciences*, *978*, 468–479.

Van Essen, D. C. (2004). Organization of visual areas in macaque and human cerebral cortex. In L. Chalupa & J. S. Werner (Eds.), *The Visual Neurosciences* (pp. 507–521). Cambridge, MA: MIT Press.

Van Essen, D. C., Dickson, J., Harwell, J., Hanlon, D., Anderson, C. H., & Drury, H. A. (2001). An integrated software system for surface-based analyses of cerebral cortex. *Journal of American Medical Informatics Association*, *8*, 443–459.

Van Essen, D. C., Felleman, D. F., DeYoe, E. A., Olavarria, J. F., & Knierim, J. J. (1990). Modular and hierarchical organization of extrastriate visual cortex in the macaque monkey. *Cold Spring Harbor Symposia in Quantitative Biology*, *55*, 679–696.

Van Essen, D. C., Harwell, J., Hanlon, D., & Dickson, J. (2004). Surface-based atlases and a database of cortical structure and function. In S. H. Koslow & S. Subramaniam (Eds.), *Databasing the Brain: From Data to Knowledge (Neuroinformatics)*. New York: John Wiley & Sons, NJ (in press).

Van Essen, D. C., Maunsell, J. H. R., & Bixby, J. L. (1981). The middle temporal visual area in the macaque: Myeloarchitecture, connections, functional properties and topographic organization. *Journal of Comparative Neurology*, *199*, 293–326.

Van Essen, D. C., Newsome, W. T. N., & Bixby, J. L. (1982). The pattern of interhemispheric connections and its relationship to extrastriate visual areas in the macaque monkey. *Journal of Neuroscience*, *2*, 265–283.

Van Essen, D. C., Newsome, W. T., Maunsell, J. H. R., & Bixby, J. L. (1986). The projections from striate cortex (V1) to areas V2 and V3 in the macaque monkey: Asymmetries, areal boundaries, and patchy connections. *Journal of Comparative Neurology*, *244*, 451–480.

Van Essen, D. C., & Zeki, S. M. (1978). The topographic organization of rhesus monkey prestriate cortex. *Journal of Physiology*, *277*, 193–226.

Van Oostende, S., Sunaert, S., Van Hecke, P., Marchal, G., & Orban, G. A. (1997). The kinetic occipital (KO) region in man: An fMRI study. *Cerebral Cortex*, *7*, 690–701.

Wade, A. R., Brewer, A. A., Rieger, J. W., & Wandell, B. A. (2002). Functional measurements of human ventral occipital cortex: Retinotopy and color. *Philosophical Transactions of the Royal Society*, *357*, 963–973.

Walker, A. E. (1940). A cytoarchitectural study of the prefrontal areas of the macaque monkey. *Journal of Comparative Neurology*, *73*, 59–86.

Watson, J. D. G., Myers, R., Frackowiak, R. S. J., Hajnal, J. V., Woods, R. P., Mazziotta, J. C., et al. (1993). Area V5 of the human brain: Evidence from a combined study using positron emission tomography and magnetic resonance imaging. *Cerebral Cortex*, *3*, 37–94.